BASIC RULES OF BEHAVIOUR OF BIVALENT METALS FLUOSILICATE HEXAHYDRATES UNDER PRESSURE

S. K. Asadov, I. M. Vitebskii, E. A. Zavadsky, V. I. Kamenev, K. V. Kamenev, B. M. Todris

Donetsk Physico-Technical Institute of the Ukrainian Academy of Sciences, 340114 Donetsk, Ukraine

Basing on the found peculiarities in behaviour of bivalent metal fluosilicate hexahydrates (M-FSH) under pressure, a generalized $P-T$ phase diagram of their crystalline states has been constructed, high-pressure phases have been identified and behaviour of M-FSH magnetic properties at superlow temperatures has been explained.

The $P-T$ diagrams of M-FSH of magnesium [1–2], manganese [3–4], iron [5–6], cobalt [7–8], nickel [8] and zinc [2] illustrate not only the unique combination of properties and phenomena typical of the above M-FSH, but the unique variety in the behaviour of different M-FSH under pressure. However, despite essential differences in the $P-T$ diagram structure, we can point to several elements of structure wich are the components of each diagram. The complex of elements in configuration shown in the Figure is the generalized $P-T$ phase diagram of M-FSH.

One of those elements are the lines of direct and inverse first-order phase transition (PT) between the high- temperature, having the elements of crystal-lattice symmetry $\bar{3}m$ ($R\bar{3}m$ for Mg-, Fe-FSH, or $P\bar{3}m1$ for Mn-FSH) state and the low-temperature monoclinic state $P2_1/c$. At the generalized $P-T$ diagram these lines are denoted as ab and $a'b'$ and run parallel to the P axis because of the transition temperature independence of pressure.

The second element is the triple point formed by the lines of three first-order PT. This point experiences the hysteresic displacements and is shown by b and b' at $P-T$ diagram. On the average, its P and T coordinates can be taken equal to 210 MPa and 300 K for Mg-FSH, 90 MPa and 235 K for Mn-FSH, 7.5 MPa and 225 K for Fe-FSH.

The third element is the part of the boundary of monoclinic phase $P2_1/c$ initiation at point of its most pronounced curvature. This is like bdk at $P-T$ diagram. The peculiar form of this line is due to the existence of critical pressure P_c, above which under sample cooling the $P2_1/c$ phase does not occur. For Mn-FSH P_c is 120 MPa, for Fe-FSH — 63 MPa and for Co-FSH — 50 MPa.

Finally, the fourth element is the line dm of second-order PT between α and β states with trigonal symmetry of crystal lattice differing in values of thermal-expansion coefficients.

The $P-T$ diagram of each M-FSH can be graphically represented as a part of generalised $P-T$ diagram to the right of the vertical line corresponding to a specific M-FSH. When going from M-FSH of one metal to that of another, from left to right, the lines are arranged to the extent of triple point pressure and critical pressure P_c decrease which was observed experimentally. For Mg-FSH, pressure corresponding to triple-point equals 210 MPa, for Mn-FSH — 90 MPa and for Fe-FSH — 7.5 MPa. In Co-FSH the triple point is not observed, but $P_c = 50$ MPa. In case of Ni- and Zn-FSH, already at atmospheric pressure, the second-order PT between trigonal phases with different values of thermal-expansion coefficient is observed, whereas in other M-FSH it occurs at $P > P_c$.

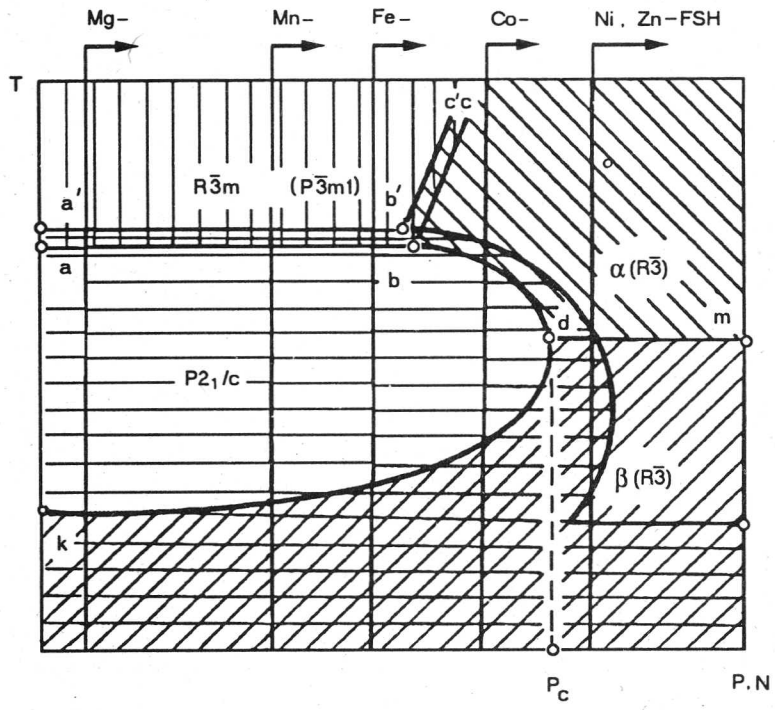

Fig. Generalized $P-T$ phase diagram of bivalent metal fluosilicate hexahydrates

As is seen from the Figure, the series M-FSH formed in the result of such an arrangement repeats the location of their corresponding bivalent metals M in periodic table. This means that there exists the relation between the shape of $P-T$ diagram of each M-FSH and the ordinal number N of incoming metal M, according to which the increase of the ordinal number of metal in M-FSH is equivalent to the displacement of the origin of its $P-T$ diagram, at the generalized $P-T$ diagram, towards higher pressures.

In M-FSH, only low-pressure phases realized in the sample at atmospheric pressure have been identified experimentally. Direct determination of symmetry of phases existing only under the uniform compression (of high- pressure phases) is impossible because of technical difficulties. However, as is seen from the generalized $P-T$ diagram, the regions of existence of high-pressure phases of some M-FSH superimpose on the regions of existence of the identified low-pressure phases of other M-FSH. The structure of generalized $P-T$ diagram shows the similarity of $P-T$ diagrams of M-FSH of high ordinal number of M and section of $P-T$ diagram for M-FSH with lower ordinal number of M which makes it possible to conclude that phases with the coincident regions of existence at the generalized $P-T$ diagram should be identical from the point of view of crystallography, in particular, α and β phases, which are the high-pressure ones for Mn-, Fe- and Co-FSH (for Mn-FSH there were no studies of the crystal structure at pressures higher than 120 MPa) should be of the same crystal structure as the low-pressure phases in Ni- and Zn-FSH, i.e. the $R\bar{3}$ structure. To confirm this statement, the following arguments can be given:

1. From the Figure it follows that the $P-T$ diagrams of Ni-FSH and of Co-FSH previously compressed up to $P > P_c$ are similar. According to the data of X-ray investigations [9], in Co-FSH and Ni-FSH the high-temperature high-pressure phases are the isostructural ones. And since the temperature behaviour of these M-FSH is identical when intersecting the *dm* line (value of the temperature expansion factor is changed) then it can be said that the isostructural are the low-temperature β-phases in Ni-FSH and the low-temperature high-pressure β-phase in Co-FSH. In Ni-FSH α- and β-phase are symmetrically identical and refer to the space group $R\bar{3}$ [10]. So, it can be supposed that the low-temperature high-pressure beta-phase in Co-FSH is also of symmetry space group $R\bar{3}$.

2. According to the Figure, the line of monoclinic phase $P2_1/c$ initiation in Mg-, Mn-, Fe-FSH can be separated into two parts. One of them, at the boundary of phase $R\bar{3}m$ ($P\bar{3}m1$) is a section of line *ab* parallel to the axis of pressure. To the right, it is limited by the triple point. The second one, *bdk*, starts with the triple point and is the boundary to the high-pressure α- and β-phases of specific curvature resulting in the formation of the *abdk* region closed at the temperature axis. Of similar curvature is the line of $P2_1/c$ phase initiation in Co-FSH at the boundary to low-pressure phase $R\bar{3}$ and high-pressure one, β-phase which is of the $R\bar{3}$ symmetry space group, as it was shown previously. This analogy again results in the conclusion that α- and β-high-pressure phases in Mg-, Mn-, Fe-FSH are identical to $R\bar{3}$ and β-phases in Co-FSH, respectively, and are the two structural type modifications of $R\bar{3}$ differing by the values of the coefficient of temperature expansion of the crystal lattice, so at the Figure they are denoted as $\alpha(R\bar{3})$ and $\beta(R\bar{3})$.

Availability of the critical pressure P_c at the generalized $P-T$ diagram means, in particular, that Mn-FSH and Co-FSH samples cooled down to superlow temperatures at $P < P_c$ will be of the monoclinic crystal structure $P2_1/c$, and at $P > P_c$ — the rhombohedral structure $R\bar{3}$. It is seen that change of the type of superlow-temperature ordering from the antiferromagnetic, when sample is cooled at $P > P_c$, to ferromagnetic, when cooling occurs at $P > P_c$, evident at magnetic $P-T$ phase diagrams, is the secondary effect with respect to structure changes showing that the antiferromagnetic ordering is typical of the $P2_1/c$ state, whereas the ferromagnetic one — of $R\bar{3}$ state. At superlow temperatures, Ni-FSH possesses only one symmetry modification $R\bar{3}$, and the $P2_1/c$ phase does not occur at all. To confirm the above correspondence between structural and magnetic properties of M-FSH it must be said that crystal of this salt orders only ferromagnetically at superlow temperatures independent of pressure influencing it under cooling [12].

1. *Gorev M. V., Flerov I. N., Aleksandrov K. S.*, Fiz. Tverd. Tela. 33, 2210 (1991).
2. *Asadov S. K., Zavadsky E. A., Kamenev V. I., Kamenev K. V., Todris B. M.*, Fiz. i Teh. Vis. Davl. 2, 104 (1992).
3. *Asadov S. K., Zavadsky E. A., Kamenev V. I., Kamenev K. V., Todris B. M.*, Fiz. i Teh. Vis. Davl. 2, 140 (1992).
4. *Asadov S. K., Zavadskii E. A., Kamenev V. I., Kamenev K. V., Todris B. M.*, XXIV Meeting on Low-Temperature Physics. Booklet of abstracts, P.3.— Kazan.— 1992.— T. 28.
5. *Asadov S. K., Zavadsky E. A., Kamenev V. I., Kamenev K. V., Todris B. M.*, Fiz. Tverd. Tela. 32, 2420 (1990).
6. *Asadov S. K., Zavadsky E. A., Kamenev V. I., Kamenev K. V., Todris B. M.*, Fiz. i Teh. Vis. Davl. 1, 7 (1991).
7. *Asadov S. K., Zavadsky E. A., Kamenev V. I., Kamenev K. V., Todris B. M.*, Theses of papers, XXVI All-Union Meeting on Low-Temperature Physics.— Donetsk.— 1990.— P.2.— p. 110.

8. *Asadov S. K., Zavadsky E. A., Kamenev V. I., Kamenev K. V., Todris B. M.*, Ukr. Fiz. Zhurnal. 36, 293 (1991).
9. *Ray S., Zalkin A. and Templeton D.*, Acta Cryst. B 29, 2741 (1973).
10. *Kodera E., Torii A., Osaki K., and Watanabe T. J.*, Phys. Soc. Japan. 32, 863 (1972).
11. *Dyakonov V. P., Zubov E. Ye., Fita I. M.*, XXV All- Union Meeting on Low-Temperature Physics. Theses of papers, P. 2.— Leningrad.— 1988.— p. 110–111.
12. *Baryuchtar V. G., Vitebsky I. M., Galkin A. A., Dyakonov V. P., Fita I. M., Tsintsadze G. A.*, Sov. Phys. JETP 84, 1083 (1983).